THE BELL SYSTEM TECHNICAL JOURNAL
Vol. 60, No. 1, January 1981
Printed in U.S.A.

High-Frequency Behavior of Waveguides with Finite Surface Impedances

By C. DRAGONE

(Manuscript received January 25, 1980)

We derive the modes inside a cylindrical waveguide of finite surface impedances, assuming the waveguide transverse dimensions are large compared to the wavelength λ. This paper restricts its consideration to the modes with $\beta \approx k$, where β is the propagation constant and $k = 2\pi/\lambda$. For these modes we show that asymptotically, for large values of k, the field ψ becomes infinitesimal (of the same order of 1/k) at the boundary. Taking this into account, we obtain simple expressions for the asymptotic properties of ψ for large k. The theory applies to a variety of waveguides: corrugated waveguides, optical fibers, waveguides with smooth walls of lossy metal, and so on. An important property of the modes considered here is that their attenuation constant is very low, i.e., asymptotic to $1/k^2$ for large k. Thus, these modes are useful for long-distance communication. Another consequence of $\psi \to 0$ at the boundary is that for large k the distribution of ψ inside the boundary is essentially independent of the boundary parameters, i.e., independent of the surface impedances in the longitudinal and transverse directions. This consequence implies that the same radiation characteristics of the corrugated feed can be obtained using other structures and, therefore, construction can be simplified in many cases, with little sacrifice in performance. We also derive general expressions for ψ and the propagation constant β.

I. INTRODUCTION

It is known[1-8] that in certain waveguides the field becomes, under certain conditions, very small at the boundary. Consider, for instance, a corrugated waveguide of radius a and let λ be the free-space wavelength. This waveguide is characterized at the boundary by finite surface impedance Z_z in the longitudinal direction. The frequency dependence of Z_z, which is determined by the depth of the corrugations, causes the transverse field distribution $\psi(x, y)$ of a mode to vary with the frequency $k = 2\pi/\lambda$. However, this frequency dependence virtually disappears (for all modes except surface waves) if the waveguide dimensions are large enough. In fact, one finds that $\psi(x, y)$ approaches for $ka \to \infty$ a frequency independent distribution that vanishes at the boundary.[5] This behavior is responsible for the low attenuation constant, for the excellent radiation characteristics, and the wide bandwidth of corrugated waveguides.[5] We show here that the same behavior also occurs, under quite general conditions, in a variety of uncorrugated waveguides.[1-21] Figures 1a and 1b show two examples, a dielectric waveguide[7,8,13-16] of general cross section and a hollow waveguide with metal walls coated by a dielectric layer.[4,17] Other examples can be obtained by modifying the boundary conditions in a variety of different ways. For instance, several dielectric layers may be used in Fig. 1b, or a metal grid of transverse wires may be placed at the boundary, as pointed out in Section II. Other examples are the waveguides of dielectric or lossy metal considered in Ref. 2. We now outline the main assumptions.

Consider a cylindrical waveguide with an interior region of homogeneous and isotopic material, as in Fig. 1c. Let Z and k be the wave impedance and propagation constant for a plane wave in the interior region, and let C denote the boundary. Then

$$Z = \sqrt{\frac{\mu}{\epsilon}}, \qquad k = \omega\sqrt{\epsilon\mu}. \tag{1}$$

Consider a mode with propagation constant β and let $\mathbf{E}_t$ denote the transverse component of the electric field,

$$\mathbf{E}_t = \psi(x, y)e^{-j\beta z}. \tag{2}$$

Let $2a$ be a characteristic dimension of the waveguide, for instance the width in the x direction as in Fig. 1c. We are concerned about the asymptotic behavior of $\psi(x, y)$ for large values of ka. Consideration will be restricted to the modes for which the propagation constant β approaches k, as $ka \to \infty$. Thus, we assume

$$\beta \to k \qquad \text{for} \quad ka \to \infty. \tag{3}$$

This excludes surface waves, as pointed out in the following section. Then, a property of the modes considered here is that $\mathbf{E}$ and $\mathbf{H}$ become transverse, in the limit as $ka \to \infty$,

$$\lim_{ka\to\infty} E_z = H_z = 0. \tag{4}$$

Another property is that asymptotically, per large ka, a set of linear relations exist at the boundary among the tangential components of $\mathbf{E}$

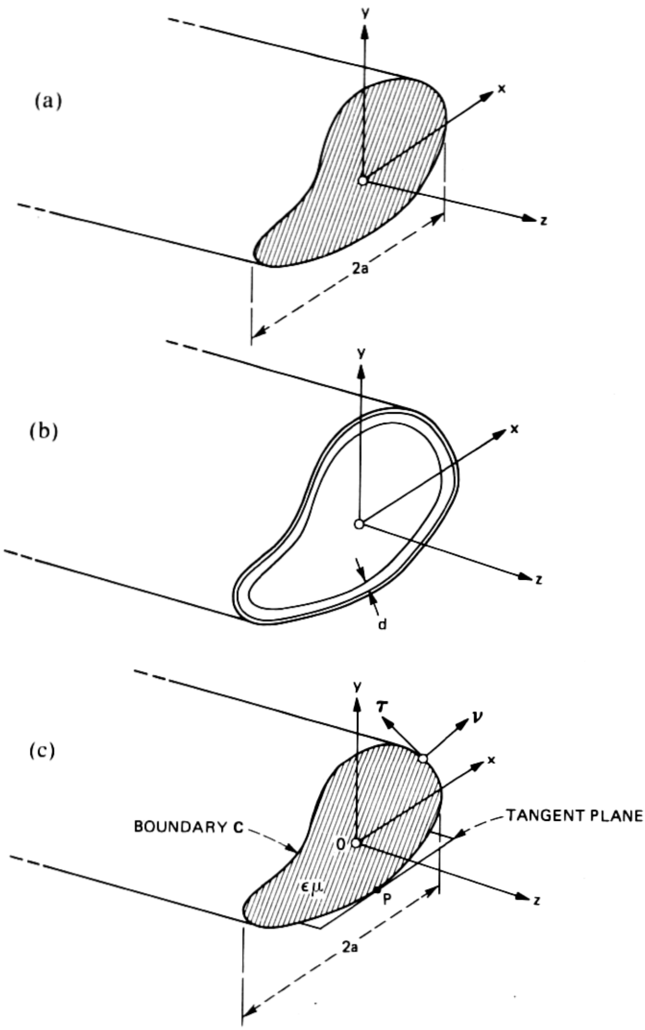

Fig. 1—Three examples of cylindrical waveguides: (a) a dielectric rod, (b) a waveguide with metal walls coated by a thin dielectric layer, and (c) a waveguide with boundary conditions shown in Fig. 2.

and **H**. It is convenient to write these relations in the form

$$\begin{bmatrix} ZH_\tau \\ E_\tau \end{bmatrix} = j[H] \begin{bmatrix} E_z \\ -ZH_z \end{bmatrix} \quad \text{on } C, \tag{5}$$

where $[H]$ is a 2×2 matrix and H_τ, E_τ denote the components of **H**, **E** in the direction of the unit vector τ in Fig. 1c. These relations together with eq. (4) give at the boundary

$$\lim_{ka\to\infty} E_\tau = H_\tau = 0 \qquad \text{on } C, \tag{6}$$

provided the matrix [H] does not diverge for $ka \to \infty$,

$$[H] \neq \infty \qquad \text{for} \quad ka \to \infty. \tag{7}$$

Throughout this article, we assume conditions (3), (5), and (7). Condition (5) is discussed in the following section, where it is pointed out that for most waveguides considered here, [H] is a diagonal matrix. In this case it is convenient to define at the boundary surface impedances Z_z and Z_τ by writing

$$E_\tau = Z_\tau H_z, \qquad E_z = -Z_z H_\tau, \tag{8}$$

where Z_z is the longitudinal impedance, and Z_τ is the transverse impedance. Then condition (7) requires

$$Z_\tau,\ 1/Z_z \neq \infty \qquad \text{for} \quad ka \to \infty. \tag{9}$$

It is important to realize that this requirement is violated in a number of cases. It is violated in a hollow waveguide with metal walls of perfect conductivity, since then $Z_z = 0$. Furthermore, in a corrugated waveguide with corrugations of depth d, the longitudinal impedance Z_z is determined by kd, and there are certain frequencies for which $Z_z = 0$. A similar situation arises in Fig. 1b where both Z_τ and Z_z vary with kd. Throughout this article it will be assumed that the quantities

$$\frac{1}{ka}, \qquad \frac{1}{ka}\frac{Z_\tau}{Z}, \qquad \frac{1}{ka}\frac{Z}{Z_z}$$

are small. Therefore, the results will not apply in the vicinity of the above frequencies.

A direct consequence of condition (6) is that the boundary values of ψ vanish, in the limit as $ka \to \infty$,

$$\lim_{ka\to\infty} \psi(x, y) = 0 \qquad \text{on } C. \tag{10}$$

Another consequence is that ψ approaches a distribution ψ_∞ independent of ka, for $ka \to \infty$. For finite ka,

$$\psi = \psi_\infty + \delta\psi, \tag{11}$$

where $\delta\psi$ (but not ψ_∞) varies with ka and

$$\lim_{ka\to\infty} \delta\psi = 0. \tag{12}$$

Notice condition (10) implies that

$$\psi_\infty = 0 \qquad \text{on } C. \tag{13}$$

These results are of practical interest for several reasons. In the design of a feed,[6] it is desirable that the boundary values of ψ be small [as implied by eq. (10)] since these values determine radiation in the side-lobes due to edge diffraction at the aperture. Furthermore, for broad-band applications, it is desirable that the frequency dependent part $\delta\psi$ of the aperture illumination be small, as implied by eq. (12). Finally, in a corrugated waveguide, or a waveguide with metal walls coated by dielectric layers, power is lost only at the walls and, therefore, it is determined by the boundary values of ψ. Since these boundary values vanish for $ka \rightarrow \infty$, the attenuation constant for the above waveguides for large ka is very small[1,2,4,18–21]; it is asymptotic to ka^{-2}. We shall see that in general ψ_∞ is independent of $[H]$ and, therefore, a variety of different waveguides, with different $[H]$ but the same boundary shape, give rise to the same ψ_∞. This explains the similarity, noted in Ref. 9, between the modes of a corrugated waveguide and those of an optical fiber, a dielectric lined waveguide,[4] and a hollow dielectric waveguide.[2] This similarity implies that essentially the same radiation characteristics of corrugated waveguides can also be obtained with a variety of other waveguides.

In the particular case of the optical fiber, some of our results are implied by the asymptotic expressions derived in Ref. 7. Exact solutions for the modes of the corrugated waveguide,[12] the optical fiber,[7,8] and the hollow waveguide of dielectric[2] are known for circular geometry. For a rectangular cross section, only approximate solutions[3,22] are known, except in special cases.[23] Exact solutions for the slab waveguide are given in Refs. 8 and 24. In all these cases one finds that condition (3) implies condition (10). Measurements of the radiation characteristics of a dielectric horn are described in Refs. 25 and 26. Some of the properties derived here apply also to propagation in stratified media.[27–29] The use of surface impedances to characterize a boundary is discussed in Ref. 30.

II. BOUNDARY CONDITIONS FOR $ka \rightarrow \infty$

We now derive and discuss eq. (5). Figure 1c shows a waveguide directed along the z axis and of general cross section in which $\boldsymbol{\nu}$ is the outwardly directed normal and $\boldsymbol{\tau}$ is a unit vector tangential to the boundary,

$$\boldsymbol{\tau} = \mathbf{i}_z \times \boldsymbol{\nu}. \tag{14}$$

The medium inside the boundary is assumed to be homogeneous and isotropic. Let C denote the closed contour of the boundary in the plane $z = 0$.

We are concerned with the properties of $\psi(x, y)$ in a waveguide of large transverse dimensions. Thus, consider a mode propagating in the waveguide of Fig. 1b and suppose the width $2a$ is increased keeping the dielectric thickness d fixed. The resulting behavior of $\psi(x, y)$ as $ka \rightarrow \infty$ can be derived exactly in two cases, when (see Appendix C)

$$\frac{\partial \psi}{\partial y} = 0 \tag{15}$$

and when the boundary is a circle. In both cases one finds that for most of the modes $\beta \rightarrow k$, as $ka \rightarrow \infty$. For these modes, the normalized field amplitude $\psi(x, y)/\psi(0, 0)$ becomes infinitesimal at the boundary for $ka \rightarrow \infty$. For the remaining modes, those for which β does not approach k, just the opposite behavior takes place: The field becomes confined to the immediate vicinity of the walls, degenerating into a surface wave with propagation constant determined by the surface impedances of the walls. Here, consideration will be restricted to the modes satisfying condition (3). An important property of these modes is that asymptotically, for large ka, the surface impedances Z_τ and Z_z become independent of ka. In fact, if one writes

$$X = -j\frac{Z_\tau}{Z}, \qquad Y = -j\frac{Z}{Z_z}, \tag{16}$$

then in Fig. 1b

$$X \rightarrow \frac{1}{\sqrt{n^2 - 1}} \tan(\sqrt{n^2 - 1}\, kd), \tag{17}$$

$$Y \rightarrow -\frac{n^2}{\sqrt{n^2 - 1}} \frac{1}{\tan(\sqrt{n^2 - 1}\, kd)}, \tag{18}$$

as shown in Appendix C. Thus, Z_τ and Z_z depend only on the refractive index n and the thickness kd of the dielectric layer.

For a circular boundary, the above relations can be derived rigorously by expressing the field in terms of Bessel functions, and then making use of well-known expressions giving the asymptotic behavior of these functions for large arguments as in Ref. 5. They can also be derived by the following argument, which applies in general to a boundary of arbitrary shape (Fig. 1c). Consider the field in the vicinity of a boundary point P in Fig. 1c. Since ka is large, the curved boundary can be approximated locally by the tangent plane. Furthermore, since $\beta \simeq k$, the field is produced locally by a plane wave at *grazing incidence.* If one determines the law of reflection for such a plane wave, and takes into account that the plane of incidence is parallel to the z axis, one obtains[24,27] eqs. (16)–(18).

The above argument can be used to derive the asymptotic behavior of Z_z and Z_τ for a variety of other waveguides, illustrated in Fig. 2.* In case (d) the boundary is a smooth surface of lossy metal with surface

* Notice k_0 denotes k in free space.

resistance R_s. In (a) the metal surface is corrugated. In (b) the medium outside the boundary is dielectric with refractive index $n_2 < n_1$. This corresponds to the optical fiber of Fig. 1a. In (c), $n_2 > n_1$ as in Ref. 2, and, therefore, both Z_z and Z_τ are real, which implies power is lost through the boundary. Other boundaries of practical interest are obtained from Fig. 2 by placing a grid of thin wires tangent to τ on the boundary. This will cause $Z_\tau \simeq 0$ in all cases. For all these waveguides one finds, for large ka, that $[H]$ in eq. (5) is a diagonal matrix,

$$[H] = -\begin{vmatrix} Y & 0 \\ 0 & X \end{vmatrix}, \tag{19}$$

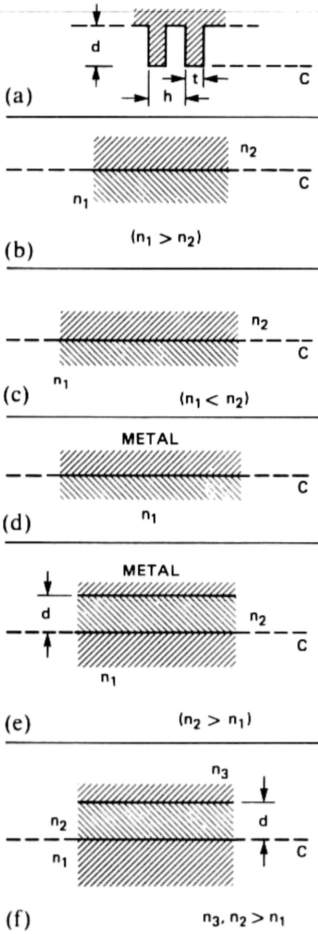

Type of boundary	Z_z	Z_τ
(a)	$jZ\left(1-\frac{t}{H}\right)\mathrm{TAN}\,K_0 d$ $(h \ll \lambda)$	$Z_t = 0$
(b)	$-j\frac{\sqrt{n_1^2-n_2^2}}{n_2}\frac{n_1}{n_2}Z$ $(Z = \sqrt{\mu/\epsilon})$	$j\frac{n_2}{\sqrt{n_1^2-n_2^2}}\frac{n_1}{n_2}Z$
(c)	$r\frac{n_1}{n_2}Z$ $(r = \sqrt{n_2^2-n_1^2}/n_2)$	$\frac{1}{r}\frac{n_1}{n_2}Z$
(d)	$(1+j)R_s$	$(1+j)R_s$
(e)	$jr\frac{n_1}{n_2}ZT + R_s(1+T^2)$ $(T = \mathrm{TAN}\,K_0\sqrt{n_2^2-n_1^2}\,d,$ $\frac{R_s}{Z} \ll T, 1/T)$	$j\frac{1}{r}\frac{n_1}{n_2}ZT +$ $+ R_s(1+T^2)$
(f)	$r\frac{n_1}{n_2}Z\frac{T'+jT}{1+jTT'}$ $\left(T' = \frac{\sqrt{n_3^2-n_1^2}}{\sqrt{n_2^2-n_1^2}}\frac{n_2^2}{n_3^2}\right)$	$\frac{1}{r}\frac{n_1}{n_2}Z\frac{T'+jT}{1+jTT'}$ $\left(T' = \frac{\sqrt{n_2^2-n_1^2}}{\sqrt{n_3^2-n_1^2}}\right)$

Fig. 2—Asymptotic values of the surface impedances Z_z and Z_τ for different boundary conditions.

and the coefficients X and Y are determined by the surface impedances given in Fig. 2. Notice there are cases where $[H]$ is not a diagonal matrix, as pointed out in Section VIII.

In the following sections we consider a waveguide with boundary conditions given by eq. (5) and derive simple expressions for the dependence of $\psi(x, y)$ upon the matrix $[H]$. These expressions are obtained neglecting terms of order higher than $1/ka$ and, therefore, they do not require an exact knowledge of $[H]$, but only of the asymptotic behavior of $[H]$, which can be determined as seen in this section. In Appendix A, a procedure for determining ψ to any desired accuracy is pointed out, but the procedure requires that $[H]$ be known accurately. Any desired accuracy for $[H]$ can be obtained by a procedure of successive approximations, but the resulting expressions are in general too complicated to be of practical interest.

Concerning the validity of the following derivation, it is important to realize that even though the expressions obtained for ψ will not satisfy the actual boundary conditions exactly, the errors will be small, of order two in $1/ka$. These errors imply the conditions satisfied at the boundary by the expressions in question can be obtained, from the actual conditions, by small perturbations, of order two in $1/ka$.

III. ASYMPTOTIC PROPERTIES OF ψ

We now determine the dependence of $\psi(x, y)$ upon the matrix $[H]$. To this purpose, it is convenient to assume that $[H]$ is independent of ka. The expressions obtained for $\psi(x, y)$ will depend on the coefficients of $[H]$. By substituting for these coefficients the expressions obtained in Section II, one obtains the dependence of ψ upon ka in general, for a waveguide with frequency dependent $[H]$.

Thus, consider a waveguide characterized by a given matrix $[H]$, and let

$$\sigma^2 = k^2 - \beta^2. \tag{20}$$

Let $\psi(x, y)$ and σ^2 be expanded in power series of l/ka,

$$\psi = \psi_\infty(x, y) + \sum_{i=1}^{\infty} \frac{1}{(ka)^i} \psi_i(x, y), \tag{21}$$

$$\sigma^2 = \sigma_\infty^2 \left(1 + \sum_{i=1}^{\infty} \frac{c_i}{(ka)^i} \right) \tag{22}$$

where the distributions ψ_∞, ψ_1, etc., are independent of ka; they are determined entirely by the shape of the boundary and the coefficients of [H].

Using eqs. (21) and (22) one can derive from eq. (5) for large ka (see Appendix A) a set of linear relations involving ψ and the normal derivative $\partial\psi/\partial\nu$,

$$\left.\begin{matrix}\psi_\nu \\ \\ \psi_\tau\end{matrix}\right] = \frac{1}{k}[H]\left.\begin{matrix}\dfrac{\partial\psi_\nu}{\partial\nu} \\ \dfrac{\partial\psi_\tau}{\partial\nu}\end{matrix}\right] + O[k^{-2}] \qquad \text{on } C. \tag{23}$$

Expressing ψ_ν and ψ_τ in terms of the x- y-components of ψ, we obtain

$$\left.\begin{matrix}\psi_x \\ \\ \psi_y\end{matrix}\right] = \frac{1}{k}[A]\left.\begin{matrix}\dfrac{\partial\psi_x}{\partial\nu} \\ \dfrac{\partial\psi_y}{\partial\nu}\end{matrix}\right] + O[k^{-2}] \qquad \text{on } C, \tag{24}$$

where

$$[A] = \begin{bmatrix}\nu_x, & \nu_y \\ -\nu_y, & \nu_x\end{bmatrix}[H]\begin{bmatrix}\nu_x, & -\nu_y \\ \nu_y, & \nu_x\end{bmatrix}, \tag{25}$$

ν_x and ν_y being the direction cosines of $\boldsymbol{\nu}$.

3.1 Derivation of ψ_∞ and c_1

We now show that for each nondegenerate eigenvalue σ_∞ there are in general two modes, characterized by different values of c_1. For most waveguides, $[H]$ has the diagonal form (19), and in this case we shall see that ψ_∞ is linearly polarized. Furthermore, if the boundary has an axis of symmetry, then the polarization vector $\mathbf{i}$ of ψ_∞ is either parallel or orthogonal to the symmetry axis. Very simple expressions are obtained in this case for ψ_∞, c_1, ψ_1. More difficult is the treatment for degeneracy of order $N > 1$. Then, in order to determine ψ_∞, one must find the $2N$ latent roots of a certain characteristic equation.

The function ψ must satisfy the wave equation,

$$\nabla_t^2\psi + \sigma^2\psi = 0, \tag{26}$$

∇_t being the transverse part of ∇. Equation (24) implies that the boundary values of ψ vanish in the limit as $k \to \infty$.* It is, therefore, convenient to represent ψ in terms of the eigenfunctions f_1, f_2, etc., that satisfy the boundary condition

$$f_r = 0 \qquad \text{on } C. \tag{27}$$

Let u_r be the eigenvalue of f_r,

$$\nabla_t^2 f_r + u_r^2 f_r = 0. \tag{28}$$

From equations (21) and (22) for $k \to \infty$, one has

$$\psi \to \psi_\infty, \qquad \sigma \to \sigma_\infty, \tag{29}$$

---

* From now on the waveguide dimensions will be kept fixed, as k is increased.

and, therefore, ψ_∞ must satisfy the wave equation with σ replaced by σ_∞. Furthermore, from eq. (24),

$$\psi_\infty = 0 \qquad \text{on } C. \tag{30}$$

Therefore, σ_∞ must be one of the eigenvalues u_r. Let

$$\sigma_\infty = u_1 \tag{31}$$

and suppose there is degeneracy of order N, so that N distinct eigenfunctions $f_1, \cdots, f_N$ correspond to the same eigenvalue. Then

$$u_1 = \cdots = u_N \tag{32}$$

and ψ_∞ can be written in the form

$$\psi_\infty = \sum_{m=1}^{N} \alpha_{xm} f_m(x, y)\, \mathbf{i}_x + \sum_{m=1}^{N} \alpha_{ym} f_m(x, y)\, \mathbf{i}_y, \tag{33}$$

involving N eigenfunctions and $2N$ coefficients α_{xm}, α_{ym}. We now show that these coefficients cannot be chosen arbitrarily, but there are in general only $2N$ possible choices corresponding to $2N$ distinct modes.

3.2 Values of α_{xm}, α_{ym}

The values of ψ at any point (x', y') inside the boundary are related to the boundary values through the integral relation[24, 32]

$$\psi(x', y') = \int_C \psi(x, y) \frac{\partial G}{\partial \nu}\, dl, \tag{34}$$

where $G = G(x, y; x', y')$ is Green's function satisfying the equation

$$\nabla_t^2 G + \sigma^2 G = \delta(x - x')\delta(y - y') \tag{35}$$

and the boundary condition $G = 0$ when x, y is a point of C. Let G be represented in terms of the eigenfunctions f_r,

$$G = \sum_1^\infty \frac{1}{\sigma^2 - u_r^2} f_r(x, y) f_r(x', y'), \tag{36}$$

where it is assumed that f_r are properly normalized so that they are real functions satisfying

$$\iint_S f_r^2(x, y)\, dxdy = 1 \qquad (r = 1, 2, \cdots), \tag{37}$$

S being the region inside the boundary C. From eq. (36), G contains a component

$$G_\infty = \frac{1}{\sigma^2 - \sigma_\infty^2} \sum_1^N f_r(x, y) f_r(x', y'), \tag{38}$$

which diverges for $k \to \infty$, since $\sigma \to \sigma_\infty$. For large k,

$$G_\infty = ka \frac{1}{\sigma_\infty^2} \frac{1}{c_1} \sum_1^N f_r(x, y) f_r(x', y'). \tag{39}$$

The asymptotic behavior of eq. (34) for large k is now examined. Approximating G by G_∞, from eqs. (24), (25), and (34) one obtains the integral relation

$$\left.\psi_\infty\right] = \frac{1}{k} \int_C [A] \left.\frac{\partial \psi_\infty}{\partial \nu}\right] \frac{\partial G_\infty}{\partial \nu}\, dl, \tag{40}$$

where

$$\left.\psi_\infty\right] = \left.\begin{matrix} \psi_{\infty x} \\ \psi_{\infty y} \end{matrix}\right]. \tag{41}$$

Substituting eq. (39) in eq. (40), and taking into account eq. (33), one obtains for the coefficients α_{xm}, α_{ym} the characteristic equation

$$\left.\begin{matrix} \alpha_x] \\ \alpha_y] \end{matrix}\right] c_1 = \begin{bmatrix} [I_{xx}] & [I_{xy}] \\ [I_{yx}] & [I_{yy}] \end{bmatrix} \left.\begin{matrix} \alpha_x] \\ \alpha_y] \end{matrix}\right], \tag{42}$$

where

$$\alpha_x] = \left.\begin{matrix} \alpha_{x1} \\ \vdots \end{matrix}\right], \qquad \alpha_y] = \left.\begin{matrix} \alpha_{y1} \\ \vdots \end{matrix}\right], \tag{43}$$

and

$$(I_{xx})_{i,s} = \frac{a}{\sigma_\infty^2} \int_C A_{xx} \frac{\partial f_s}{\partial \nu} \frac{\partial f_i}{\partial \nu}\, dl, \tag{44}$$

and similarly for I_{xy}, I_{yx}, I_{yy} (replace A_{xx} with A_{xy}, A_{yx}, A_{yy}).

Equation (42) admits, in general , a total of $2N$ independent solutions $\alpha_1]$, $\alpha_2]$, $\cdots$, $\alpha_{2N}]$ for

$$\alpha] = \left.\begin{matrix} \alpha_x] \\ \alpha_y] \end{matrix}\right]. \tag{45}$$

Each solution is obtained by solving eq. (42) with c_1 set equal to one of the $2N$ latent roots $\lambda_1, \lambda_2, \cdots, \lambda_{2N}$ of the matrix

$$[I] = \begin{bmatrix} [I_{xx}] & [I_{xy}] \\ [I_{yx}] & [I_{yy}] \end{bmatrix}. \tag{46}$$

If the boundary is lossless, then one can verify that $[I]$ is Hermitian and its latent roots are *real.* In this case the $2N$ solutions are orthogonal,

$$\alpha_i]\alpha_s]_t^* = 0 \qquad \text{for} \quad i \neq s, \tag{47}$$

where $(\ )_t^*$ denotes the transpose conjugate.

Thus, to determine the coefficients α_{x1}, α_{y1}, etc., which specify ψ_∞, the $2N$ latent roots of the matrix $[I]$ must be determined. If the roots are all distinct, then they correspond to $2N$ distinct modes characterized by different c_1, i.e., by different propagation constant β. If there is degeneracy ($N > 1$), the expressions obtained from eq. (33) for ψ_∞ are quite complicated. Much simpler is the treatment for $N = 1$, since then only one eigenfunction $f_1(x, y)$ is involved. This is the most important case in practice, since it applies to the fundamental modes, which correspond to the lowest σ_∞ (see Appendix B).

3.3 Case N = 1

For $N = 1$, only one eigenfunction $f_1(x, y)$ corresponds to σ_∞ and eq. (33) reduces to

$$\psi_\infty = f_1(x, y)\mathbf{i}, \tag{48}$$

where $\mathbf{i}$ is a unit vector that determines the polarization of ψ_∞. If $\lambda_1 \neq \lambda_2$, then eq. (42) for $N = 1$ specifies two polarizations, corresponding to two modes with different propagation constants. To determine these two polarizations, let α_x and α_y be the direction cosines of $\mathbf{i}$. Then from eq. (42) with $N = 1$,

$$\begin{bmatrix} I_{xx} - c_1 & I_{xy} \\ I_{xy} & I_{yy} - c_1 \end{bmatrix} \begin{bmatrix} \alpha_x \\ \alpha_y \end{bmatrix} = 0, \tag{49}$$

where

$$I_{xx} = \frac{a}{\sigma_\infty^2} \int_C A_{xx} \left[\frac{\partial f_1}{\partial \nu}\right]^2 dl, \tag{50}$$

and similarly for I_{xy}, I_{yx}, I_{yy} (replace A_{xx} with A_{xy}, etc.). From eq. (49) one obtains for c_1 the characteristic equation

$$(I_{xx} - c_1)(I_{yy} - c_1) = I_{xy}I_{yx}, \tag{51}$$

whose solutions λ_1 and λ_2 determine for $\mathbf{i}$ two eigenvectors $\mathbf{i}_1$ and $\mathbf{i}_2$ with direction cosines specified by eq. (49). Notice $\mathbf{i}_1 = \mathbf{i}_2$ if $\lambda_1 \neq \lambda_2$. If the boundary is lossless and $\lambda_1 \neq \lambda_2$, then from eq. (47)

$$\mathbf{i}_1 \cdot \mathbf{i}_2^* = 0, \tag{52}$$

and, therefore, the two eigenvectors represent orthogonal polarizations.

For all the waveguides of Fig. 2, $[H]$ is given by eq. (19). Then

$$I_{xy} = I_{yxx} = -\frac{a}{\sigma_\infty^2} \int_C (Y - X)\nu_x\nu_y \left[\frac{\partial f_1}{\partial \nu}\right]^2 dl, \tag{53}$$

$$I_{xx} = -\frac{a}{\sigma_\infty^2} \int_C (Y\nu_x^2 + X\nu_y^2) \left[\frac{\partial f_1}{\partial \nu}\right]^2 dl, \tag{54}$$

and similarly for I_{yy} (interchange $x \rightleftarrows y$). Since in this case $[I]$ is a symmetric matrix,

$$\mathbf{i}_1 \cdot \mathbf{i}_2 = 0, \tag{55}$$

and if $\mathbf{i}_1$ is real (ψ_∞ is linearly polarized), then $\mathbf{i}_2$ is also real and orthogonal to $\mathbf{i}_1$.

We conclude by deriving a general condition that must be satisfied so that ψ_∞ is linearly polarized. Suppose $\mathbf{i}$ is real. Then the x axis can be oriented so that $\mathbf{i} = \mathbf{i}_x$. This implies $\alpha_y = 0$ and therefore $I_{yx} = 0$. We conclude that linear polarization is obtained only if it is possible to orient the x axis so that

$$\int_C (Y - X)\nu_x\nu_y\left[\frac{\partial f_1}{\partial \nu}\right]^2 dl = 0. \tag{56}$$

Notice then $I_{xy} = I_{yx} = 0$, and, therefore,

$$\mathbf{i}_1 = \mathbf{i}_x, \qquad \mathbf{i}_2 = \mathbf{i}_y. \tag{57}$$

The above requirement is always satisfied if the boundary is lossless (then X and Y are real) or if the values of X and Y are independent of position l on the boundary. It is also satisfied if the boundary has an axis of symmetry. In fact, let the symmetry axis be the x axis. Then X, Y and $\partial f_1/\partial\nu$ in eqs. (53) and (54) are even functions of y,

$$X(x, y) = X(x, -y), \qquad Y(x, y) = Y(x, -y), \tag{58}$$

whereas $\nu_x\nu_y$ is an odd function of y, which gives condition (56).

We thus conclude that in most cases of practical interest ψ_∞ is linearly polarized. This is of importance in the design of a feed for reflector antennas, to obtain good cross-polarization discrimination over a wide frequency range.

IV. PROPAGATION CONSTANT FOR $N = 1$

Assume the boundary has an axis of symmetry given by the x axis and let $N = 1$. Let $[H]$ be given by eq. (19), which applies to all waveguides of Fig. 2. Then, for the mode polarized in the x direction, the coefficient c_1 coincides with I_{xx} and it is given by eq. (54). Notice eq. (54) assumes that $f_1(x, y)$ is normalized as shown by eq. (37). If f_1 is not normalized, we must divide the right-hand side of eq. (54) by the left-hand side of eq. (37) with $r = 1$, then obtaining

$$c_1 = ja\,\frac{\displaystyle\int_C (Z_\tau\,\nu_y^2/Z + Z\nu_x^2/Z_z)\;(\partial f_1/\partial\nu)^2\,dl}{\displaystyle u_1^2\iint f_1^2\,dxdy} \tag{59}$$

for $\mathbf{i} = \mathbf{i}_x$. For the other polarization $\mathbf{i} = \mathbf{i}_y$, interchange $\nu_y \rightleftarrows \nu_x$ in the above expression, which shows that the two polarizations are in general characterized by different propagation constants.

Once c_1 is known, the propagation constant β can be derived using eqs. (20) and (22) which for $\sigma_\infty = u_1$ give

$$\beta = k - \frac{1}{2}\frac{u_1^2}{k} - \frac{1}{2}\frac{u_1^2}{k^2 a} c_1 + \cdots, \tag{60}$$

where the dots indicate terms of order higher than two in $1/k$. If the medium inside the waveguide is lossless, k is real and the attenuation constant η is determined by the imaginary part of c_1. Then eqs. (59) and (60) give

$$\eta = -\mathrm{Im}(\beta) = \frac{\int_C (r\nu_y^2 + g\nu_x^2)(\partial f_1/\partial \nu)^2 \, dl}{2k^2 \iint f_1^2 \, dx dy}, \tag{61}$$

where r and g are the real parts of Z_τ/Z and Z/Z_z. This relation was used in Ref. 1 to determine the attenuation constant for a variety of waveguides of practical interest.

Using the above expressions one can straightforwardly calculate the dispersion and attenuation characteristics of any mode for large ka. In the special case of a hollow waveguide of dielectric with circular boundary, eqs. (59) and (60) give eq. (31) of Ref. 2.

Of greatest importance are the fundamental modes, which correspond to the lowest σ_∞. Then, for the circular boundary of Fig. 3,

$$f_1(x, y) = AJ_0(\sigma_\infty \rho), \tag{62}$$

where $\rho = \sqrt{x^2 + y^2}$, J_0 is the Bessel function of order zero, and $\sigma_\infty a$ is the first root of J_0,

$$\sigma_\infty a = 2.4048. \tag{63}$$

For the rectangular boundary of Fig. 3,

$$f_1(x, y) = A \cos\left(\frac{\pi}{2}\frac{x}{a}\right) \cos\left(\frac{\pi}{2}\frac{y}{b}\right). \tag{64}$$

If $f_1(x, y)$ is normalized [see eq. (37)], then

$$A = \begin{cases} \dfrac{1}{a\sqrt{\pi}} \dfrac{1}{J_1(\sigma_\infty a)} & \text{(circle)}, \\[2ex] \dfrac{1}{\sqrt{ab}} & \text{(rectangle)}. \end{cases} \tag{65}$$

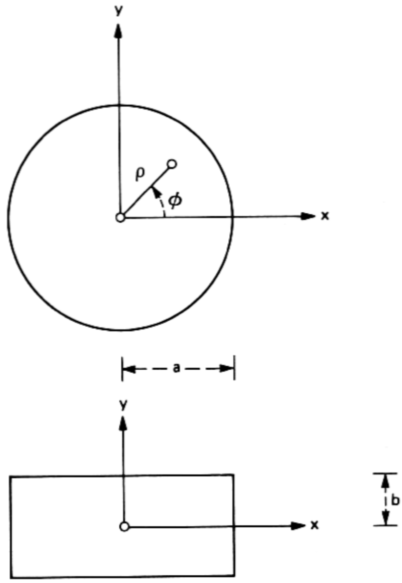

Fig. 3—Circular and rectangular boundaries.

V. THE DISTRIBUTION ψ_1

Once ψ_∞ is known, the boundary values of ψ can be calculated with error of order two in $1/k$ using eq. (23). If $N = 1$, $\mathbf{i} = \mathbf{i}_x$ and $[H]$ is given by eq. (19), then one obtains at the boundary

$$\psi \simeq -\frac{1}{k}\left[(X\nu_y^2 + Y\nu_x^2)\mathbf{i}_x - (X - Y)\nu_x\nu_y\mathbf{i}_y\right]\frac{\partial f_1}{\partial \nu} \qquad \text{on } C. \qquad (66)$$

To determine ψ inside the boundary we separate ψ into two parts, a component

$$f_1(x, y)\mathbf{i},$$

plus a component due to the other eigenfunctions f_2, f_3, etc. The latter component can be determined with error of order two in $1/k$ by substituting eq. (66) in the integral of eq. (34), with G replaced by $G - G_\infty$ for $\sigma = \sigma_\infty$, as shown in Appendix A. Concerning the former component, it is shown in Appendix A that if the boundary has an axis of symmetry, then $\mathbf{i}$ is independent of k, and, therefore, one can set $\mathbf{i} = \mathbf{i}_x$ for all values of k. If there is no symmetry, then in general $\mathbf{i}$ is a function of k and, to determine its dependence upon k, one must follow the same procedure used in this section to determine $\mathbf{i}$ for $k \to \infty$.

VI. APPLICATIONS

We now derive the fundamental modes of circular and rectangular boundaries with diagonal matrix $[H]$ given by eq. (19), which applies to all the waveguides of Fig. 2. The surface parameters X and Y will be assumed to be independent of position on the boundary. Then for $\mathbf{i} = \mathbf{i}_x$,

$$\psi_\infty = f_1(x, y)\mathbf{i}_x, \qquad (67)$$

giving ψ in the limit as $k \to \infty$. We now wish to obtain a better approximation for ψ.

For the rectangular boundary of Fig. 3b in eq. (66), one has $\nu_x \nu_y = 0$, and, therefore, ψ has the same polarization as ψ_∞, i.e.,

$$\psi \simeq \psi \mathbf{i}_x,$$

neglecting terms of order two in $1/k$. The boundary condition (23) can then be satisfied separating ψ into a product of two functions, $\psi_1(x)$ and $\psi_2(y)$, subject to the conditions

$$\psi_1 = -\frac{Y}{k}\frac{\partial \psi_1}{\partial \nu} \quad \text{for} \quad x = \pm a, \qquad (68)$$

$$\psi_2 = -\frac{X}{k}\frac{\partial \psi_2}{\partial \nu} \quad \text{for} \quad y = \pm b, \qquad (69)$$

whose solutions are well known.[26–31] For the fundamental mode one obtains

$$\psi = A \cos \alpha x \cos \gamma y, \qquad (70)$$

where

$$\alpha a = \frac{\pi}{2}\left[1 - \frac{Y}{ka} + \cdots\right], \qquad \gamma b = \frac{\pi}{2}\left[1 - \frac{X}{kb} + \cdots\right]. \qquad (71)$$

These results are closely related to expressions derived in Ref. 3 for a dielectric waveguide. Notice that for $b \to \infty$ the rectangular waveguide degenerates into two parallel plates placed at $x = \pm a$, in which case $\psi \to \psi_1(x)$ and the modes can be derived exactly as in Appendix C. Similarly, for $a \to \infty$ one obtains two plates at $y = \pm b$ and $\psi \to \psi_2(y)$. If both a and b are finite, then eq. (70) shows that ψ is simply the product of the two distributions $\psi_1(x)$ and $\psi_2(y)$, provided terms of order two in $1/k$ can be neglected.

Next consider the circular waveguide of Fig. 3. In this case it is convenient to introduce polar coordinates ρ, ϕ. Taking into account that X and Y are independent of ϕ, one obtains for the fundamental mode

$$\psi = A\left\{J_0(\sigma\rho)\mathbf{i}_x - \frac{X - Y}{4}\frac{(\sigma_\infty a)^2}{ka} J_2(\sigma\rho)(\cos 2\phi \mathbf{i}_x + \sin 2\phi \mathbf{i}_y) + \cdots\right\}, \qquad (72)$$

where the dots indicate terms of order two in $1/k$, and from eqs. (22) and (59),

$$\sigma a = \sigma_\infty a \left[1 - \frac{X + Y}{2} \frac{1}{ka} + \cdots \right], \tag{73}$$

$\sigma_\infty a$ being given by eq. (63). These expressions were derived previously for $X = 0$ in Ref. 5 and therefore details of their derivation are not given here.

The above results for rectangular and circular waveguide are valid provided k is large enough so that the field at the boundary is small. From eq. (66) this requires

$$\frac{1}{ka} \ll 1, \qquad \frac{X}{ka} \ll 1, \qquad \frac{Y}{ka} \ll 1.$$

If the waveguide dimensions are large enough, the results apply even to an ordinary waveguide with metal walls of finite conductivity. To determine how large the dimensions must be, consider for instance copper at 100 GHz. Then $R_s/Z = 2.189 \times 10^{-4}$, and from Fig. 2d one obtains $|Y| = 514$ and $|X| = 5 \times 10^{-5}$. Therefore, the above inequalities require

$$2a \gg 1000\lambda,$$

which is too large a diameter for all practical purposes.

The above requirement is a consequence of the large value of Y for copper walls. By coating the walls with a thin dielectric layer, or by corrugating them, much lower values of Y can be obtained. Suppose for instance in Fig. 2e one chooses $T = 1$, $R_s \approx 0$, $n_1 = 1$, and $n_2^2 = 2$. Then, instead of the above requirement, one obtains $a \gg 0.318\lambda$, which is a much more realistic condition. The attenuation constant of such a waveguide, or of other waveguides realized using one of the structures of Fig. 2, can be determined straightforwardly using eq. (61).[1]

When a waveguide is used to illuminate a feed aperture, then at that aperture usually $ka \gg 1$. Then the aperture illumination is given accurately by eqs. (70) or (72) for rectangular and circular apertures. For other apertures, it can be determined as pointed out in Section V. By deriving the Fourier transform of eqs. (70) and (72) the far-field can be determined and thus its dependence on the aperture parameters X and Y can be obtained. These applications are discussed in Ref. 1.

Helical waveguide—A case where [H] is not a diagonal matrix

Consider one of the waveguides of Fig. 2, and let a helical wire be placed at the boundary, as in Fig. 4. Then one finds that $[H]$ is not a

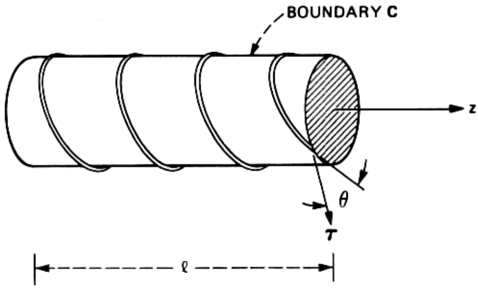

Fig. 4—Helix with pitch angle θ.

diagonal matrix,

$$[H] = \frac{-1}{\cos^2\theta - XY\sin^2\theta} \cdot \begin{bmatrix} Y, & j\sin\theta\cos\theta(1+XY) \\ -j\sin\theta\cos\theta(1+XY), & X \end{bmatrix}, \quad (74)$$

where X, Y denote the coefficients of $[H]$ for $\theta \to 0$, θ being the pitch angle between the wire and τ.

Consider a circular boundary. Then, we have seen that for $\theta = 0$ the fundamental modes have the same propagation constant, and are linearly polarized for $k \to \infty$. In this section we show that for $\theta \neq 0$ they become circularly polarized, and have different propagation constants β_1 and β_2. This implies the following. Suppose at the input of such a waveguide (Fig. 4) the fundamental modes are combined so as to obtain, to a good approximation, linearly polarized excitation. Then, one will not obtain, in general, linear polarization at the output, unless the difference between the two propagation constants is small enough so that

$$(\beta_2 - \beta_1)l \ll \frac{\pi}{8},$$

l being the waveguide length. In this section we derive β_2 and β_1. Helical waveguides are of importance for their simplicity of construction, as compared to corrugated waveguides, and for their excellent performance as hybrid-mode feeds, as shown recently by R. H. Turrin[33] whose work motivated the calculation of this section. The following results agree with Ref. 34.

Let consideration be restricted to the fundamental modes of a lossless boundary with $[H]$ independent of position on the boundary. Then, from eqs. (25) and (44)

$$I_{xx} = H_{11}\nu_{xx} - (H_{12} + H_{21})\nu_{xy} + H_{22}\nu_{yy}, \quad (75)$$

$$I_{xy} = (H_{11} - H_{22})\nu_{xy} + H_{12}\nu_{xx} - H_{21}\nu_{yy}, \quad (76)$$

and similarly for I_{yx} and I_{yy} (interchange $1 \rightleftarrows 2$, $x \rightleftarrows y$), where

$$\nu_{jk} = \frac{1}{\sigma_\infty^2} \int_C \nu_j \nu_k \left| \frac{\partial f_1}{\partial \nu} \right|^2 dl \qquad (j, k = x, y). \tag{77}$$

Since the boundary is assumed to be lossless,

$$(\mathrm{Im})(I_{xy}) = H_{12}(\nu_{xx} + \nu_{yy}), \tag{78}$$

and, therefore, $I_{xy} \neq 0$. We conclude that for $H_{12} \neq 0$ there is no degeneracy possible for the fundamental modes. For a circular boundary, using eqs. (74), (25), (50), (51), and (62), we obtain

$$\mathbf{i} = \frac{1}{\sqrt{2}} (\mathbf{i}_x \pm j\mathbf{i}_y) \tag{79}$$

and

$$\sigma a = \sigma_\infty a \left[1 - \frac{1}{2(\cos^2\theta - XY \sin^2\theta)} \cdot \left(\frac{X + Y}{ka} \mp 2 \sin\theta \cos\theta \frac{1 + XY}{ka} \right) + \cdots \right], \tag{80}$$

with the plus sign of eq. (79) corresponding to the minus sign of eq. (80). The same expressions apply also to a square aperture with $a = b$. Thus, in both cases ψ_∞ is circularly polarized. If $XY + 1 > 0$, then the lower value of σ corresponds to a mode with polarization rotating in the sense of the helix in Fig. 4. The opposite is true for $XY + 1 < 0$.

VII. CONCLUSIONS

To summarize, we have shown for most of the modes inside a cylindrical waveguide of finite surface impedances that asymptotically, for large values of ka, the field ψ vanishes at the boundary. We have seen in Section III that for each eigenvalue u_r there are, in general, $2N$ modes, given for $k \to \infty$ by eq. (33). For the lowest eigenvalue one has $N = 1$, and for the corresponding two modes ψ_∞ is given by $f_1(x, y)\mathbf{i}$, where $\mathbf{i}$ is a unit vector. If the direction cosines of $\mathbf{i}$ are complex, then ψ_∞ is elliptically polarized. If $[H]$ is a diagonal matrix, as for the waveguides of Fig. 2, and the boundary has an axis of symmetry, then $\mathbf{i}$ is real, and one can always orient the x axis so that $\mathbf{i} = \mathbf{i}_x$. In this case the propagation constant β is given by eqs. (59) and (60), and using the procedure of Appendix A we can straightforwardly determine ψ, with error of order two in $1/k$, for any boundary shape. For rectangular and circular boundaries ψ is given by eqs. (70) and (72).

Of special importance are the fundamental modes, which correspond to the lowest eigenvalue σ_∞. These modes, treated in Section 3.2, are needed in reflector antennas to minimize cross-polarization and edge illumination over the feed aperture. They are also needed for long distance waveguide or fiberguide communication. Our results, show that there is no need to corrugate the walls of a feed in order to obtain conditions (11) and (48) or to obtain the low attenuations calculated in Refs. 20 and 21. Furthermore, they imply that the low attenuations predicted in Ref. 2 for a hollow waveguide of dielectric, or for a waveguide with metal walls coated with dielectric,[4] can be achieved also using other waveguides. These applications are discussed in Ref. 1.

APPENDIX A

A.1 Derivation of eq. (23)

Taking into account that $\nabla \cdot \mathbf{E} = 0$, one can express E_z in terms on the transverse component given by eq. (2). One obtains

$$E_z = \frac{e^{-j\beta z}}{j\beta} \nabla_t \psi.$$

Using this relation and Maxwell's equation $-j\omega\mu\mathbf{H} = \nabla \times \mathbf{E}$ one can express H_z and $\mathbf{H}_t$ in terms of ψ. Substituting these expressions in eq. (5), we obtain the boundary condition

$$\begin{bmatrix} \psi_\nu \\ \\ \psi_\tau \end{bmatrix} = \frac{1}{k}[H] \begin{bmatrix} \dfrac{k}{\beta}(\nabla_t \psi) \\ \\ -\nabla_t \cdot (\mathbf{i}_z \times \psi) \end{bmatrix} + \begin{bmatrix} \dfrac{1}{\beta^2}\dfrac{\partial}{\partial \nu}(\nabla_t \cdot \psi) \\ \\ 0 \end{bmatrix}. \tag{81}$$

Taking into account eqs. (21) and (22) for $k \to \infty$, we have

$$\psi \to 0, \qquad \text{on} \quad C.$$

This implies

$$\nabla_t \cdot \psi \to \frac{\partial \psi_\nu}{\partial \nu}, \qquad \nabla_t \times \psi \to \mathbf{i}_z \frac{\partial \psi_\tau}{\partial \nu}.$$

Taking into account these relations, from eq. (81) we obtain eq. (23) with error of order two in $1/k$.

A.2 Development of σ^2 and ψ in Asymptotic Series of $1/ka$

A general procedure for deriving the various terms c_r, ψ_r in eqs. (21) and (22) is now described, thus justifying these equations. Assume that the boundary has at least one line of symmetry, since this simplifies considerably the derivation, and it applies to most cases of practical interest. Also assume that $[H]$ has the diagonal form of eq. (19), and that a single eigenfunction $f_1(x, y)$ corresponds to σ_∞.

Since there is no degeneracy, ψ_∞ is given by eq. (48). Let the x axis coincide with the symmetry line. Then, the surface parameters X and

Y are even functions of y,

$$X(x, -y) = X(x, y) \qquad \text{and} \qquad Y(x, -y) = Y(x, y), \tag{82}$$

and we now show the modes can be divided in two groups, namely *even modes* satisfying

$$\psi_x(x, -y) = \psi_x(x, y), \qquad \psi_y(x, -y) = -\psi_y(x, y), \tag{83}$$

and *odd modes* satisfying

$$\psi_x(x, -y) = -\psi_x(x, y), \qquad \psi_y(x, -y) = \psi_y(x, y). \tag{84}$$

In fact, let

$$\boldsymbol{\psi} = \psi_x(x, y)\mathbf{i}_x + \psi_y(x, y)\mathbf{i}_y$$

be a solution of the wave equation and of the boundary condition (81) with $[H]$ given by eq. (19). Then we wish to show that

$$\boldsymbol{\psi}' = \psi_x(x, -y)\mathbf{i}_x - \psi_y(x, -y)\mathbf{i}_y$$

is also a solution. Notice that $\boldsymbol{\psi}'$ is the *image* of $\boldsymbol{\psi}$ with respect to the x axis, as shown in Fig. 5, where P and P' denote two corresponding points (x, y) and $(x, -y)$. One can verify that

$$(\nabla_t \times \boldsymbol{\psi}')_{P'} = -(\nabla_t \times \boldsymbol{\psi})_P, \tag{85}$$

$$(\nabla_t \boldsymbol{\psi}')_{P'} = (\nabla_t \boldsymbol{\psi})_P. \tag{86}$$

If P is a boundary point, and $\boldsymbol{\nu}'$ and $\boldsymbol{\nu}$ denote the normals to the boundary at P' and P, respectively, one has that $\boldsymbol{\nu}'$ is the *image* of $\boldsymbol{\nu}$ because the boundary is symmetrical. Taking all this into account one can verify that $\boldsymbol{\psi}'$ satisfies the boundary condition (81) with $[H]$ given by eq. (19) at P'. We conclude that if an arbitrary solution $\boldsymbol{\psi}$ is known, two independent solutions $\boldsymbol{\psi}_e$ and $\boldsymbol{\psi}_o$ can be obtained by the relations

$$\boldsymbol{\psi}_e = \tfrac{1}{2}[\boldsymbol{\psi} + \boldsymbol{\psi}'], \qquad \boldsymbol{\psi}_o = \tfrac{1}{2}[\boldsymbol{\psi} - \boldsymbol{\psi}']. \tag{87}$$

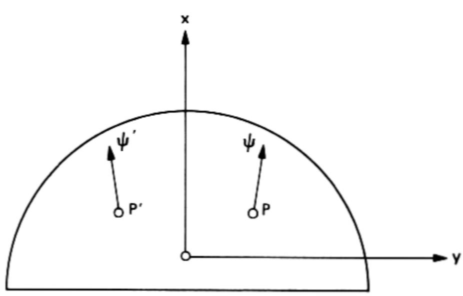

Fig. 5—For a symmetrical boundary, the boundary conditions are satisfied by both $\boldsymbol{\psi}$ and its mirror image $\boldsymbol{\psi}'$.

One solution, ψ_e, is *even* and the other, ψ_o, is *odd*.

We now proceed to derive σ^2 and ψ. Let $\mathbf{i} = \mathbf{i}_x$ and assume $f_1(x, y)$ is even, i.e.,

$$f_1(x, y) = f_1(x, -y), \tag{88}$$

all other cases ($\mathbf{i} = \mathbf{i}_y$, or f_1 odd) being entirely analogous. Then ψ_x and ψ_y are, respectively, even and odd and it is convenient to separate G into three parts,

$$G = G_\infty + G_x + G_y, \tag{89}$$

where G_x, G_y denote, respectively, the even and odd parts of $G - G_\infty$.* Taking into account that ψ_x is even, from eqs. (34), (36), and (89) one obtains

$$\psi_x = A_1 f_1(x, y) + \int_C \psi_x \frac{\partial G_x}{\partial \nu} dl, \tag{90}$$

where

$$A_1 = \frac{1}{\sigma^2 - u_1^2} \int_C \psi_x \frac{\partial f_1}{\partial \nu} dl. \tag{91}$$

Similarly, for ψ_y,

$$\psi_y = \int_C \psi_y \frac{\partial G_y}{\partial \nu} dl. \tag{92}$$

In eq. (90), since ψ can be multiplied by an arbitrary constant, the coefficient A_1 can be chosen arbitrarily. We choose $A_1 = 1$, to be consistent with $\psi_\infty = f_1(x, y)\mathbf{i}_x$. Then eq. (91) gives

$$\sigma^2 - \sigma_\infty^2 = \int_C \psi_x \frac{\partial f_1}{\partial \nu} dl, \tag{93}$$

a basic relation that expresses σ^2 in terms of the boundary values of ψ_x. Expanding ψ_x in a power series of $1/ka$, from eq. (91) one obtains for the ith coefficient of σ^2,

$$c_i = \frac{1}{\sigma_\infty^2} \int_C \psi_{xi} \frac{\partial f_1}{\partial \nu} dl, \tag{94}$$

where ψ_{xi} is the x component of ψ_i in eq. (21). From eq. (66),

$$\psi_{x1} = -(X\nu_y^2 - Y\nu_x^2) a \frac{\partial f_1}{\partial \nu}, \tag{95}$$

* Thus G_y is obtained from eq. (36) considering only those terms for which f_r are odd, whereas for G_x, consideration is restricted to f_r even with $r > 1$.

and, therefore, for $i = 1$, eq. (94) gives eq. (59).

From eqs. (90) and (92), taking into account that at the boundary $\delta\psi = \psi - \psi_\infty = \psi$,

$$\delta\psi_x = \int_C \delta\psi_x \frac{\partial G_x}{\partial \nu}\, dl, \qquad \delta\psi_y = \int_C \delta\psi_y \frac{\partial G_y}{\partial \nu}\, dl. \tag{96}$$

Thus, using eq. (95), we obtain

$$\psi_{x1} = -\int_C (X\nu_y^2 + Y\nu_x^2) \frac{\partial f_1}{\partial \nu} \left(\frac{\partial G_x}{\partial \nu}\right)_\infty dl, \tag{97}$$

for the values of ψ_{x1} inside the boundary whereas for ψ_{y1}, using eq. (66), we obtain

$$\psi_{y1} = \int_C \nu_x \nu_y (x - Y) \frac{\partial f_1}{\partial \nu} \left(\frac{\partial G_y}{\partial \nu}\right)_\infty dl, \tag{98}$$

where $(\ )_\infty$ denotes the value for $\sigma = \sigma_\infty$. Equations (97) and (98) allow ψ and its derivatives to be determined with an error $O(1/k)$. Therefore, the right-hand side of eq. (81), which contains the factor $1/k$, can now be calculated with an error $O(1/k^2)$. The boundary values of ψ_{x2}, ψ_{y2} are then obtained from eq. (81).

Once these values are known, eq. (96) can be used to determine ψ_{x2} and ψ_{y2} inside the boundary. Equation (81) can then be used again to determine the boundary values of ψ_{x3} ψ_{y3}, whose values inside the boundary can then be calculated using eq. (96). By proceeding this way, we can successively calculate all ψ_{xi}, ψ_{yi}. Notice in eq. (96) that the kernels depend on σ^2. Therefore, to determine ψ_{xi}, ψ_{yi} for $i > 1$, we must first calculate the coefficients $c_1, \cdots, c_{i-1}$ using eq. (94). Once these coefficients are known, the kernels must be developed in power series of $1/k$, and then the first $i - 1$ terms in these series must be determined. These terms then allow eq. (96) to be used to determine ψ_{xi}, ψ_{yi}.

APPENDIX B

Let f_1 be one of the eigenfunctions satisfying the boundary condition $f_1 = 0$ and the wave equation

$$\nabla_t^2 f_1 + u_1^2 f_1 = 0,$$

and let u_1 be the lowest eigenvalue. This implies that if $g(x, y)$ is an arbitrary function with continuous derivatives, then

$$\iint_S g \nabla_t^2 g\, dxdy \le u_1^2 \iint_S g^2\, dxdy, \tag{99}$$

where the inequality sign applies to any $g(x, y)$ that is not an eigenfunction corresponding to the eigenvalue u_1.

Condition (99) is now used to show that f_1 cannot have nodal lines inside S. In fact, suppose f_1 has a nodal line inside S, and let

$$g = |f_1|.$$

Then, since $\nabla_t g$ is discontinuous across the nodal line, g cannot be an eigenfunction, and, therefore, condition (99) should give an inequality. To evaluate the integral

$$I = \iint g\nabla_t^2 g \, dxdy \tag{100}$$

in the immediate vicinity of the nodal line, where $\nabla_t^2 g$ diverges because of the discontinuity of $\nabla_t g$, write

$$g\nabla_t^2 g = \nabla_t[g\nabla_t g] - (\nabla_t g)^2$$

and notice that

$$g\nabla_t g$$

is continuous because $g = 0$ on the nodal line. It follows that $g\nabla_t^2 g$ does not diverge on the nodal line, and, therefore, its integral over a narrow strip containing the nodal line vanishes as the width of the strip goes to zero. Thus,

$$I = \iint_S f_1 \nabla_t^2 f_1 \, dxdy = u_1^2 \iint_S f_1^2 \, dxdy \tag{101}$$

and, therefore, condition (99) gives an equality, which implies f_1 cannot have nodal lines inside S.

It is now shown that f_1 is the only eigenfunction corresponding to u_1. In fact, if f_2 is another eigenfunction corresponding to u_1, then this must be true also for

$$f = f_1 + \alpha f_2,$$

where α is an arbitrary constant. But this is not possible, since one can always choose α causing f to have a nodal line inside S, and we have already seen that this violates condition (99).

APPENDIX C

Consider the modes propagating between two parallel planes orthogonal to the x axis and let $2a$ be the spacing of the two planes. Assume at the boundary one of the conditions of Fig. 2, and let the x axis be oriented in the direction of propagation, so that there is no variation in the y direction. Then

$$\psi = \psi(x)\mathbf{i}, \tag{102}$$

where $\mathbf{i}$ is a unit vector. For the TM-modes, $\mathbf{i} = \mathbf{i}_x$, whereas for the TE-modes $\mathbf{i} = \mathbf{i}_y$. For the former case $E_\tau = H_z = 0$ and, therefore, ψ is independent of the transverse impedance Z_τ. In the latter case $H_\tau = E_z = 0$ and ψ is independent of Z_z. In either case one finds[24,27] that the surface impedances Z_τ and Z_z in eq. (9) can be determined straightforwardly. For two metal plates with dielectric coating of thickness d, for instance, Z_τ and Z_z are determined entirely by β, d, and the refractive index n of the dielectric,

$$X = \frac{k}{\sqrt{k^2n^2 - \beta^2}} \tan\left(d\sqrt{k^2n^2 - \beta^2}\right), \tag{103}$$

and

$$Y = -\frac{n^2k}{\sqrt{k^2n^2 - \beta^2}} \frac{1}{\tan\left(d\sqrt{k^2n^2 - \beta^2}\right)}, \tag{104}$$

which for $\beta \to k$ give eqs. (17) and (18). Analogous expressions are obtained for the other boundaries in Fig. 2.

Consider the even modes with $\mathbf{i} = \mathbf{i}_x$,

$$\psi = \psi\mathbf{i}_x = \cos\sigma x\mathbf{i}_x, \tag{105}$$

where from eq. (81) the wavenumber σ must satisfy[31]

$$\frac{Y}{ka} = \frac{1}{\sigma a \tan\sigma a}, \tag{106}$$

whose behavior for real values of σa is illustrated in Fig. 6a. If $Y \neq \infty$, then Y/ka vanishes for $ka \to \infty$ and, therefore, for most of the solutions of eq. (106),

$$\sigma a \to m\pi - \frac{\pi}{2}, \qquad m = 1, 2, \cdots, \tag{107}$$

as $ka \to \infty$. In addition to these solutions, for $Y < 0$ one mode exists for which σa is imaginary and[31]

$$\sigma a \to -j\frac{ka}{Y}, \qquad \text{as} \quad a \to \infty. \tag{108}$$

Equation (107) implies that the boundary values of ψ vanish for $ka \to \infty$, whereas eq. (108) implies that the mode is a surface wave whose

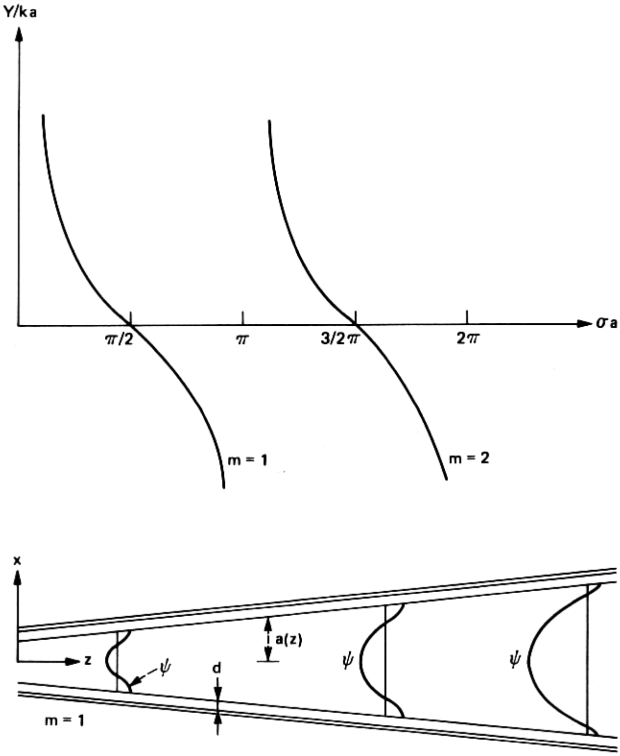

Fig. 6—Relationship between σa and Y/ka for the TM-modes of a parallel plate waveguide. Notice in the dielectric-lined waveguide the spacing $2a$ of the two plates increases with z. As a consequence, the field amplitude ψ at the boundary decreases with a, for the mode with $m = 1$.

amplitude in the vicinity of the walls is given by

$$\psi \simeq \frac{1}{2} \exp\left(+ \frac{k}{|Y|} a \right) \exp\left(- \frac{k}{|Y|} |x - a| \right). \tag{109}$$

Notice eq. (107) implies

$$\beta \to k, \tag{110}$$

as $ka \to \infty$, whereas for the surface wave

$$\beta \to k \sqrt{1 + \frac{1}{Y^2}} \neq k. \tag{111}$$

To understand the significance of these results, consider two metal plates with dielectric coating as in Fig. 1a. Let the separation a of the two plates be gradually increased in the direction of propagation, as shown in Fig. 6, and let $a \to \infty$ as $z \to \infty$. Let the dielectric thickness

d be so small that initially, for $z = 0$,

$$\frac{Y}{ka} \simeq -\infty. \tag{112}$$

Then the modes for $z = 0$ are essentially those of an ordinary waveguide without dielectric coating,

$$\sigma a \simeq m\pi \qquad (m = 0, 1, 2, \cdots). \tag{113}$$

For $z > 0$, however, the magnitude of Y/ka decreases with z, and $Y/ka \to 0$ for $z \to \infty$. This implies, for all the modes with $m \neq 0$, conditions (107) and (110) and, therefore, the boundary values of ψ vanish for $z \to \infty$. For $m = 0$, on the other hand, σa is imaginary and initially $\sigma a \simeq 0$. This mode will degenerate for $z \to \infty$ into a surface wave with propagation constant determined by Y as shown by eq. (111). This is the only mode for which the field does not become infinitesimal at the walls for $z \to \infty$. For all the other modes the boundary values of ψ for large ka are given by

$$(-1)^{m+1} Y \frac{\sigma a}{ka}, \tag{114}$$

which vanishes for $ka \to \infty$.

The above considerations apply also to the TE-modes. In fact, it can be verified that if in eq. (2) E_t is replaced with ZH_t so that ψ represents the transverse component of ZH_t, then, for the even modes, ψ is still given by eqs. (105) and (106), provided Y is replaced with X. The behavior of the odd modes is entirely analogous; simply replace $\cos \sigma x$ with $\sin \sigma x$ in eq. (105), and tan with − cotan in eq. (106).

REFERENCES

1. C. Dragone, "Attenuation and Radiation Characteristics of the HE_{11}-Mode," IEEE Trans. MTT, 7 (July 1980), pp. 704–10.
2. E. A. J. Marcatili and R. E. Schmeltzer, "Hollow Metallic and Dielectric Waveguides for Long Distance Optical Transmission and Lasers," B.S.T.J., *43*, No. 4 (July 1964), pp. 1783–1809.
3. E. A. J. Marcatili, "Dielectric Rectangular Waveguide and Directional Coupler for Integrated Optics," B.S.T.J., *48*, No. 7 (September 1969), pp. 2071–2102.
4. J. W. Carlin and P. D'Apostino, "Normal Modes in Over-Moded Dielectric-Lined Circular Waveguide," B.S.T.J., Vol. *52*, No. 4 (April 1973), pp. 453–86.
5. C. Dragone, "Reflection, Transmission, and Mode Conversion in a Corrugated Feed," B.S.T.J., *56*, No. 6 (July–August 1977), pp. 835–67.
6. C. Dragone, "Characteristics of a Broadband Corrugated Feed: A Comparison Between Theory and Experiment," B.S.T.J., *56*, No. 6 (July–August 1977), pp. 869–88.
7. A. W. Snyder, "Asymptotic Expressions for Eigenfunctions and Eigenvalues of a Dielectric or Optical Waveguide," IEEE Trans. MTT, *17* (December 1969), pp. 1130–8.
8. D. Marcuse, *Theory of Dielectric Optical Waveguides*, New York: Academic, 1974.
9. P. J. B. Clarricoats, "Similarities in the Electromagnetic Behavior of Optical Waveguides and Corrugated Feeds," Electron. Lett., *6*, No. 6 (March 1970), pp. 178–80.
10. V. H. Rumsey, "Horn Antennas with Uniform Power Patterns Around their Axes,"

IEEE Trans. Antenna Propag., *AP-14*, No. 5 (September 1966), pp. 656–8.
11. H. C. Minnett and B. MacA. Thomas, "A Method of Synthesizing Radiation Patterns with Axial Symmetry," IEEE Trans. Antenna Propag., *AP-14*, No. 5 (September 1966), pp. 654–6.
12. P. J. B. Clarricoats and P. K. Saha, "Propagation and Radiation Behavior of Corrugated Feeds; Part 1—Corrugated Waveguide Feed," Proc. IEEE, *118*, No. 9 (September 1971), pp. 1167–76.
13. S. E. Miller, E. A. J. Marcatili, and Tingye Li, "Research Toward Optical-Fiber Transmission Systems, Part I: The Transmission Medium," Proc. IEEE, *61* (December 1973), pp. 1703–51.
14. D. Gloge, "Propagation Effects in Optical Fibers," IEEE Trans. MTT, *23* (January 1975), pp. 106–20.
15. D. Marcuse, *Light Transmission Optics*, Princeton, New Jersey: Van Nostrand, 1972.
16. N. S. Kapany and J. J. Burke, *Optical Waveguides*, New York: Academic, 1972.
17. H. G. Unger, "Lined Waveguide," B.S.T.J., *41*, No. 2 (March 1962), pp. 745–68.
18. J. W. Carlin and P. D'Apostino, "Low-Loss Modes in Dielectric Lined Waveguide," B.S.T.J., *50*, No. 5 (May–June 1971), pp. 1631–9.
19. J. W. Carlin, "A Relation for the Loss Characteristics of Circular Electric and Magnetic Modes in Dielectric Lined Waveguide," B.S.T.J., *50*, No. 5 (May–June 1971), pp. 1639–44.
20. P. J. B. Clarricoats and P. K. Saha, "Attenuation in Corrugated Circular Waveguide," Electron. Lett., *6* (1970), pp. 370–2.
21. P. J. Clarricoats, A. D. Oliver, and S. L. Chang, "Attenuation in Corrugated Circular Waveguide," Parts 1 and 2: Theory and Experiment, Proc. IEEE, *122*, No. 11 (November 1975), pp. 1173–83.
22. J. E. Goell, "A Circular-Harmonic Computer Analysis of Rectangular Dielectric Waveguides," B.S.T.J., *48* (1969) pp. 2133–60.
23. R. B. Dydbal, L. Peters, and W. H. Peake, "Rectangular Waveguide with Impedance Walls," IEEE Trans. MTT, *19*, No. 1 (January 1971), pp. 2–9.
24. R. E. Collin, *Field Theory of Guided Waves*, New York: McGraw-Hill, 1960.
25. N. Brooking, P. J. B. Clarricoats, and A. D. Oliver, "Radiation Patterns of Pyramidal Dielectric Waveguides," Electron. Lett., *10* (February 1974), pp. 33–4.
26. P. J. B. Clarricoats and C. E. R. C. Salemo, "Antennas Employing Conical Dielectric Horns," Proc. Inst. Elect. Eng., *120* (July 1973), pp. 741–9.
27. J. R. Wait, *Electromagnetic Waves in Stratified Media*, New York: Pergamon, 1970.
28. E. Bahar, "Propagation of VLF Radio Waves in a Model Earth-ionosphere Waveguide of Arbitrary Height and Finite Surface Impedance Boundaries: Theory and Experiment," Radio Sci. (New Series), *Vol. 1*, No. 8 (1966), pp. 925–38.
29. E. Bahar, "Generalized Scattering Matrix Equations for Waveguide Structures of Varying Surface Impedance Boundaries," Radio Sci., *2* (New Series), No. 3 (March 1967), pp. 287–97.
30. R. A. Waldron, "Theory of Guided Electromagnetic Waves," London: Van Nostrand, 1969.
31. V. V. Scherchenko, "Continuous Transitions in Open Waveguides," translated from Russian by P. Beckman, Boulder, Colorado: GOLEM Press, 1971.
32. A. Sommerfeld, *Partial Differential Equations in Physics*, New York: Academic, 1967.
33. R. H. Turrin, "A Helical-Wire Hybrid-Mode Conical-Horn Antenna," IREECON, Sydney, Australia, August 30, 1979.
34. S. Ghosh and G. P. Srivastava, "Corrugated Waveguide with Helically Continuous Corrugations," IEEE Trans. Antenna Propag. *AP-27*, No. 4 (July 1979), pp. 564–7.